# Ship Detection Based on Faster R-CNN Using Range-Compressed Airborne Radar Data

Tamara Loran, André Barros Cardoso da Silva, *Member, IEEE*, Sushil Kumar Joshi, *Member, IEEE*, Stefan V. Baumgartner, *Senior Member, IEEE*, and Gerhard Krieger, *Fellow, IEEE*

***Abstract*— Near real-time ship monitoring is crucial for ensuring safety and security at sea. Established ship monitoring systems are the automatic identification system (AIS) and marine radars. However, not all ships are committed to carry an AIS transponder and the marine radars suffer from limited visibility. For these reasons, airborne radars can be used as an additional and supportive sensor for ship monitoring, especially on the open sea. State-of-the-art algorithms for ship detection in radar imagery are based on constant false alarm rate (CFAR). Such algorithms are pixel-based and therefore it can be challenging in practice to achieve near real-time detection. This letter presents two object-oriented ship detectors based on the faster region-based convolutional neural network (R-CNN). The first detector operates in time domain and the second detector operates in Doppler domain of airborne Range-Compressed (RC) radar data patches. The Faster R-CNN models are trained on thousands of real X-band airborne RC radar data patches containing several ship signals. The robustness of the proposed object-oriented ship detectors is tested on multiple scenarios, showing high recall performance of the models even in very dense multitarget scenarios in the complex inshore environment of the North Sea.**

***Index Terms*— Airborne radar, deep learning, maritime safety, moving target indication (MTI), synthetic aperture radar (SAR).**

## I. Introduction

HIGH ship density and illegitimate shipping activities (e.g., piracy and illegal fishing) are ongoing challenges for coastal authorities. For enhancing the current maritime situation awareness, near real-time ship detection as a part of ship monitoring is needed. Popular and prevalent systems used for ship monitoring applications are onboard transponder based systems, such as the automatic identification system (AIS) [1] and marine radars. However, these systems have major drawbacks: 1) not all ships, especially the smaller ones, are obligated to carry an AIS transponder; 2) the reliability of transponder-based systems depends on the cooperation of the ships; and 3) the marine radars are limited by their acquisition range. To overcome these shortcomings, air- and spaceborne radars have been used as additional data sources. These radars offer great potential for ship monitoring due to their ability to cover wide areas and acquire high-resolution data independent of prevailing weather and daylight conditions [1], [2], [3]. Unlike spaceborne radars, airborne radars can achieve both shorter revisits and longer observation times, but not at global coverage [2], [3], [4].

Conventionally, ship detection methods are based on constant false alarm rate (CFAR), which are powerful and well-known in the open literature [5]. However, they may have some drawbacks for their operational use. For instance, in high-resolution radar data, a single ship can be composed of thousands of detected pixels. Therefore, after detection, additional postprocessing (e.g., clustering) becomes necessary to come up with ship objects, which increases the computation time. Furthermore, since most CFAR-based algorithms operate on single pixels but not objects, a number of false detections may be obtained from other marine objects or from high-intensity ocean clutter. An additional postprocessing may be needed afterward for reducing the number of false detections [5], [6].

Recent studies have shown that the application of deep learning techniques for ship detection can be a great alternative with very promising results [7], [8], [9]. In particular, the faster region-based convolutional neural network (R-CNN) [10] is currently one of the most employed deep learning frameworks for ship detection in radar imagery [8].

Most deep learning techniques developed for ship detection are primarily applied on fully focused synthetic aperture radar (SAR) images. SAR image generation is a time-consuming process and is generally not suitable for ship detection with real-time capability. One potential solution for achieving future real-time ship detection capability is the use of Range-Compressed (RC) radar data. Unlike in fully focused SAR images, for RC data, no range cell migration correction and azimuth compression using reference functions have to be carried out, which significantly reduces the overall processing time. The RC airborne radar data are even more attractive from the point of view that the signal-to-noise ratio in most cases is sufficiently large, and they allow for long observation times which enable continuous monitoring of hotspots. To the authors' knowledge, the applicability of deep learning techniques to RC radar data for ship detection has not yet been intensively investigated [11].

In this letter, two novel deep learning methodologies are proposed for detecting the ships using RC airborne radar data. The first framework detects the ships in time domain, while the second detects the ships in Doppler domain. The detectors are based on the Faster R-CNN framework with a ResNet-50 [12] backbone, which is well-established for

Manuscript received 9 August 2022; revised 22 October 2022 and 7 December 2022; accepted 11 December 2022. Date of publication 14 December 2022; date of current version 2 February 2023. *(Corresponding author: André Barros Cardoso da Silva.)*

The authors are with the Radar Concepts Department, Microwaves and Radar Institute, German Aerospace Center (DLR), Oberpfaffenhofen, 82234 Weßling, Germany (e-mail: andre.silva@dlr.de).

Digital Object Identifier 10.1109/LGRS.2022.3229141

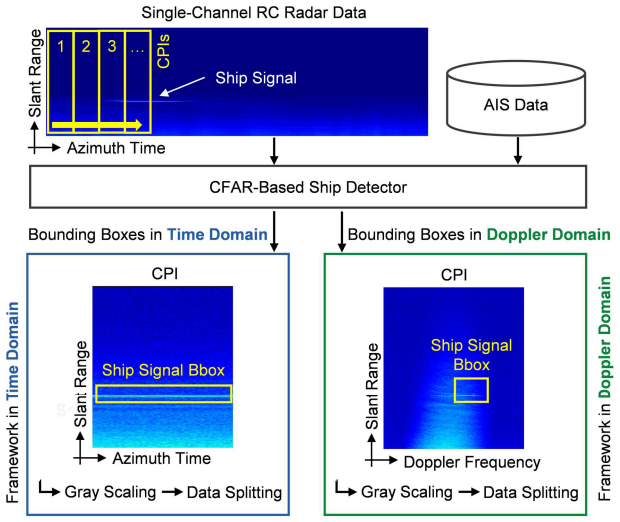


Fig. 1. Workflow used for generating the training and testing datasets in time domain and Doppler domain.

ship detection and thus provides a suitable baseline for initial investigations. They are trained and tested based on eleven real X-band RC radar datasets acquired with DLR's airborne systems F-SAR [13], [14], and DBFSAR (with digital beamforming capabilities) [15]. In addition, this letter presents a detailed comparison between the proposed detectors and a state-of-the-art CFAR-based ship detector [6].

The remainder of this letter is organized as follows. Section II describes the process of generating training and testing datasets. Section III reviews the Faster R-CNN framework. Section IV introduces the study area and the acquired datasets. Section V presents and discusses the experimental results. Section VI summarizes the results and concludes the letter.

## II. Training and Testing Datasets Generation

As a supervised algorithm, the Faster R-CNN detection framework requires labeled input data, which means that for all available RC radar datasets (c.f., Section IV), all ship signals need to be indicated in the form of radar imagery coordinates typically expressed as boundary boxes of the ship signals [10]. Due to the large amount of available RC radar data, manual labeling is not feasible. For this reason, in this letter, the CFAR-based ship detector proposed by Joshi et al. [6] is used in combination with the AIS data (c.f., Section IV) for a fully automatic large-scale labeling approach to create the necessary reference data for training and testing purposes.

Fig. 1 shows the framework used for generating the training and the testing datasets, which are required inputs for the two proposed Faster-RCNN ship detectors (c.f., Section III). First, the RC radar datasets (c.f., Section IV) are partitioned in time domain along the azimuth or flight direction into data patches known as coherent processing intervals (CPIs). The length of the CPI is system parameter dependent [6]. For instance, in this letter, each CPI contains 128 azimuth samples and all available range bins. Second, the CPIs are transformed to range-Doppler domain by applying a fast Fourier transform (FFT) along the azimuth direction, since the CFAR-based ship detector used in this letter operates in the Doppler domain [6]. Then, the CPIs are processed by the CFAR-based detector, which provides the clusters (and the boundary boxes) of the detected signals. The AIS data are then used for selecting the real ships from these clustered signals. Once the ships are verified, their corresponding signals in both time and Doppler domains are used for labeling. It is pointed out that CPIs without ship signals were discarded for training.

As shown in Fig. 1, two Faster R-CNN models need to be trained. The first model is trained for ship detection in time domain, which uses the CPIs and the corresponding boundary boxes in time domain. The second model is trained for ship detection in Doppler domain, using the CPIs and the boundary boxes in Doppler domain. For both domains, the steps "gray scaling" and "data splitting" are required. By gray scaling, the magnitude of the pixels of each CPI is converted to a magnitude range between 0 and 255 (i.e., the minimum value is assigned to 0 and the maximum value is assigned to 255). Then, in the data splitting step, the grayscaled CPIs containing several ship signals and their associated boundary box labels are assigned to one of the three datasets: training, validation, and testing, with the respective ratio of 70%, 15%, and 15%.

Additional investigations were carried out regarding the benefits of using a pretrained model instead of training the Faster R-CNN models from scratch. Therefore, a Faster R-CNN model, which was trained on microsoft common objects in context (COCO) [16], was investigated for the time and Doppler domain. However, after fine-tuning the model for each domain, no benefit occurred.

## III. Faster R-CNN Ship Detectors

As a two-stage detection model, the Faster R-CNN detector predicts in the first step regions where an object might be located. In the second step, a regression and classification are carried out to retrieve the accurate object boundary box and its object category [10]. Single-stage detectors, in contrast, locate, classify, and predict the object boundary box in a single step, whereby these detectors tend to be faster due to their lower complexity. Hence, they are often used if the hardware is limited or the processing time is critical. However, since there is a trade-off between accuracy and time, single-stage detectors are known to be less accurate than the two-stage detectors [8].

The Faster R-CNN [10] ship detectors were implemented with PyTorch. As the backbone of the Faster R-CNN models the well-established ResNet-50 [12] CNN was chosen, which is known to achieve high accuracy [8]. Training and testing of the Faster R-CNN detectors in time and Doppler domain were carried out on a processing server equipped with a Tesla V100 SXM2 32GB graphics card by using a single GPU. Over 31 306 CPIs containing ship signals from 57 ships (with AIS transponders) were used for training and testing the proposed detectors. The models were trained over 60 epochs.

For evaluating the accuracy of the implemented Faster R-CNN detectors (c.f., Table I), the following metrics are used [17]:

$$p = \frac{\mathrm{TP}}{\mathrm{TP} + \mathrm{FP}} \tag{1}$$

$$r = \frac{\mathrm{TP}}{\mathrm{TP} + \mathrm{FN}} \tag{2}$$

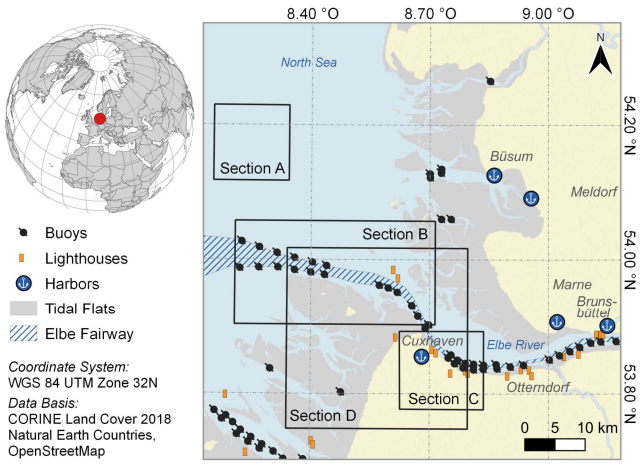


Fig. 2. Study area and the flight sections (A–D) within the Elbe river estuary at the German North Sea coast.

where TP (true positives) is the number of correctly detected ship signals, FP (false positives) is the number of signals which were incorrectly detected as a ship signal, and FN (false negatives) is the number of ship signals that were not detected.

While the precision $p$ indicates the reliability of a model in detecting the ship signals correctly, the recall $r$ identifies the effectiveness of a model in detecting ship signals by considering the missing detections (FN). A detection is considered as TP if there is a spatial overlap between the predicted bounding box and the reference bounding box (i.e., obtained from the CFAR-based detector, c.f., Section II).

To assess the overall performance of the detectors, the $F_1$-score was calculated [17]

$$F_1\text{-score} = \frac{2 \times p \times r}{p + r} \tag{3}$$

which indicates the balance between $r$ and $p$.

## IV. Study Area and Data

The study was carried out in the southeastern part of the North Sea, close to the city Cuxhaven, Germany. High-density ship traffic makes the area particularly well suited for ship detection studies. In 2016 and 2019, two flight campaigns were conducted. For the flight campaign 2016, the RC airborne radar data were acquired with DLR's F-SAR system [13], [14] and in 2019 DLR's DBFSAR [15] system was used. Both systems were mounted on a Do-228 aircraft and operated in X-band. Fig. 2 shows the flight sections A–D within the study area. These flight sections differ in complexity in terms of natural and man-made structures.

In total, 11 VV-polarized datasets were considered for this study. Eight datasets were used for training and validation, and three datasets were used as testing data. The RC radar data were acquired during linear flights and circular flights, and cover an area of about 1062 km$^2$. Fig. 3 shows the acquisition geometries of the testing datasets 1–3.

Besides the airborne RC radar data, during the flight campaigns also AIS data were acquired for evaluating the proposed ship detectors. It is pointed out that only the ships that carried an AIS transponder were considered in this letter. In total, 57 AIS transponder carrying ships could be identified within the 11 considered RC radar datasets.

## V. Experimental Results

The proposed ship detectors are tested using real X-band VV-polarized RC airborne radar data. In this section, the experimental results are presented and discussed. Table I shows the main information obtained from the 12 AIS carrying ships that were detected in the three considered testing datasets. Moreover, the accuracy metrics obtained per dataset in the time domain (c.f., Section V-A) and in the Doppler domain (c.f., Section V-B) are shown. Finally, the performance of the proposed ship detector operated in Doppler domain is compared with the state-of-the-art CFAR-based ship detector, which is proposed in [6].

### A. Proposed Ship Detector in Time Domain

As shown in Table I for dataset 1, an accuracy of 98.50% was achieved for all metrics. Such a high accuracy is explained by the low complexity of the scene. Dataset 1 was acquired offshore over flight section A, where the surrounding area of the ship BAD BRAMSTEDT was free of man-made objects.

For datasets 2–3, the accuracy metrics are lower with respect to dataset 1 due to the detection of several other man-made objects (e.g., buoys) present in the scenes. For instance, the $p$ values for datasets 2–3 were obtained as 65.87% and 27.35%, respectively. Since several other objects were counted as false detections (which raised the number of FP), the $p$ value was low. However, it was not possible to determine if such objects were indeed false detections or ships without AIS transponders. Therefore, due to the lack of ground truth validation for such objects, the $r$ values (which consider the number of FN) are considered more meaningful than the $p$ values for the complex scenarios of datasets 2–3.

Fig. 4 shows several subsequent grayscaled CPIs obtained from dataset 1 in time domain. The ship BAD BRAMSTEDT was detected in all CPIs (c.f., the ship information from AIS in Table I), so that its observation time was more than 20 s. The boundary box edges of the reference data (green), generated from the CFAR-based ship detector [6], are shown along with the predicted boundary box edges of the proposed Faster R-CNN (orange) ship detector in time domain.

The predicted boundary boxes by the proposed ship detector seem to be smooth and fit even better than the reference data itself. Note that for the reference data, the boundary boxes overestimated the ship extent in the slant range for several CPIs due to increased target signal energy as the CFAR-based algorithm detects only in range-Doppler.

### B. Proposed Ship Detector in Doppler Domain

Table I shows that for dataset 1, the accuracy metrics obtained from the ship detector operated in Doppler domain are again high due to the low complexity of the scenario, as already pointed out in Section V-A.

For datasets 2–3, lower accuracies were achieved compared to dataset 1. The detection of other objects in datasets 2–3

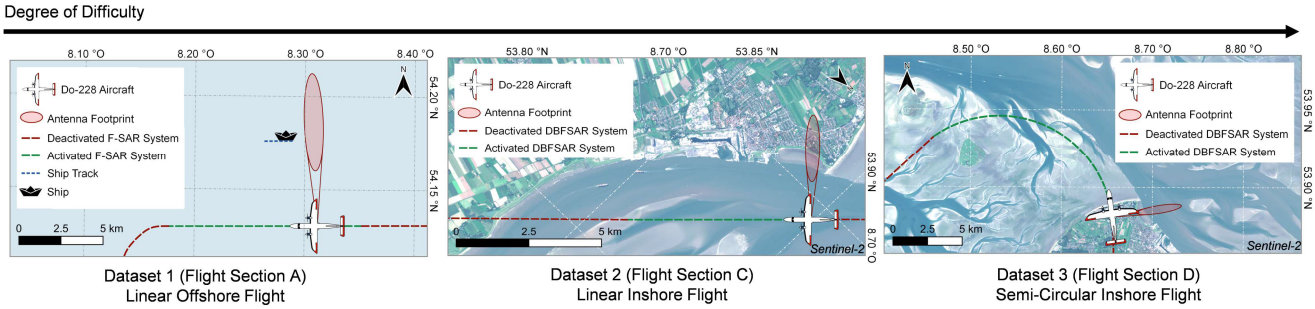


Fig. 3. Acquisition geometries of the testing datasets 1–3 corresponding to the flight sections shown in Fig. 2.

TABLE I

SHIP INFORMATION FROM THE AIS AND SUMMARY OF ACCURACY METRICS FOR THE TESTING DATASETS

| | | | | Ship Detection in Time Domain | | | Ship Detection in Doppler Domain | | |
|---|---|---|---|---|---|---|---|---|---|
| Dataset | Ship Name | Length×Width [m] | Speed [kn] | $r$ [%] | $p$ [%] | $F_1$-Score [%] | $r$ [%] | $p$ [%] | $F_1$-Score [%] |
| 1 | BAD BRAMSTEDT | 66×10 | 18.20 | 98.50 | 98.50 | 98.50 | 98.25 | 98.99 | 98.62 |
| 2 | HAM 316 | 129×22 | 7.64 | 90.61 | 65.87 | 76.28 | 83.07 | 74.41 | 78.50 |
| | LANGELAND | 82×12 | 5.87 | | | | | | |
| | LONGDUIN | 112×15 | 11.94 | | | | | | |
| | MARLIES | 17×5 | 9.51 | | | | | | |
| | STICKERS GAT | 16×6 | 11.85 | | | | | | |
| 3 | AURORA | 20×6 | 7.16 | 88.07 | 27.35 | 41.74 | 84.91 | 27.73 | 41.81 |
| | GEO GRAPH | 18×6 | 3.88 | | | | | | |
| | LONGDUIN | 112×15 | 12.01 | | | | | | |
| | PILOTVESSEL HANSE | 49×21 | 9.40 | | | | | | |
| | RMS RATINGEN | 88×11 | 8.32 | | | | | | |
| | TINA CUX-5 | 19×5 | 4.29 | | | | | | |

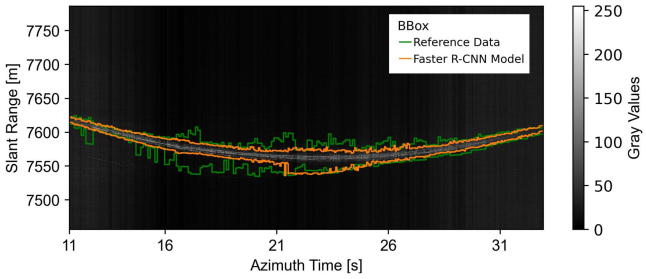


Fig. 4. Detections of the ship signal of BAD BRAMSTEDT in time domain.

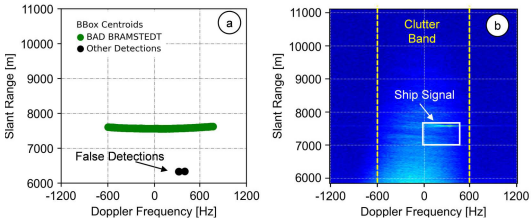


Fig. 5. (a) Detections of the ship BAD BRAMSTEDT obtained in Doppler domain by the proposed ship detector. (b) Single CPI in Doppler domain showing a ship signal within the sea clutter. Unfortunately, the sea state was not known for this data acquisition.

has again reduced the $p$ values. The proposed ship detector in Doppler domain achieved less FP and less TP in comparison with the ship detector in time domain, which lead to higher $p$ and lower $r$ values. Nevertheless, the achieved $r$ values for datasets 2–3 are sufficiently high.

As an example, Fig. 5(a) shows the detections of the ship BAD BRAMSTEDT (dataset 1) in Doppler domain. For visualization purposes, only the centroids of the predicted boundary boxes per CPI are shown. The ship was observed for over 21 s or 393 successive CPIs (c.f., Fig. 4). Since each CPI corresponds to a different acquisition time, the ship is successively detected at different Doppler frequencies. Besides, it can be seen that the proposed ship detector was able to detect the ship also within the sea clutter band [c.f., Fig. 5(b)]. It is pointed out that in case of high sea states, smaller ships may not be detected. In such cases, clutter suppression would need to be applied before detection.

### C. Comparison With CFAR-Based Ship Detector

The proposed detector in Doppler domain is compared with the CFAR-based detector [6] (which also detects the ships in Doppler domain) in terms of accuracy and processing time. The comparison is shown in Fig. 6 for dataset 2. The same behavior was observed for the other testing datasets.

Dataset 2 contains five AIS carrying ships (c.f., Table I). Fig. 6(a) shows the binary detection map obtained with the CFAR-based ship detector [6]. The detections were obtained in Doppler domain and then were mapped into time domain for visualization purposes. As it can be seen in the figure, the CFAR-based detector successfully detected all the ships in the dataset. However, several isolated false detections were also obtained due to its pixel-based approach.

Fig. 6(b) shows the improved detection results achieved by the implemented Faster R-CNN detector operated in Doppler domain. All ships were detected with less false detections in

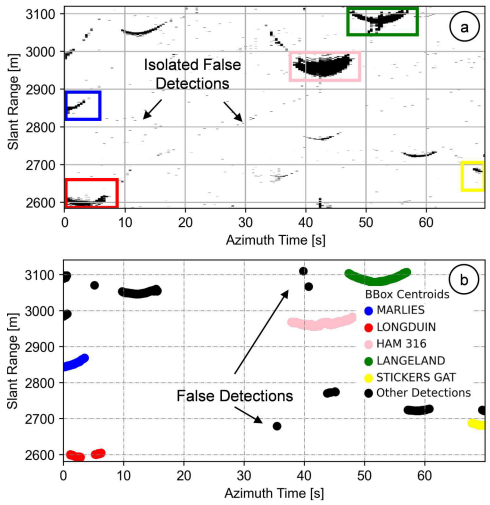


Fig. 6. Binary detection maps obtained from dataset 2 (c.f., Table I). Detections obtained from (a) CFAR-based ship detector, and (b) the proposed ship detector. Both detectors were applied in Doppler domain and, only for visualization purposes, the detections were remapped to time domain.

comparison to the CFAR-based approach. Furthermore, it can also be seen in Fig. 6(b) that the ship LONGDUIN (in red) had some missed detections. This is caused by the near range location of the ship, where the sea clutter contribution is stronger, and thus making it difficult to detect the ship within the clutter band (for instance, see Fig. 5(b), where the stronger clutter power is present in near range).

In Fig. 6(a) and (b), besides the AIS carrying ships, other objects have been detected that might be ships without AIS transponders or other man-made objects (e.g., buoys).

For ship monitoring applications, high detection accuracy and low processing time are important. Therefore, also the processing time required by the CFAR-based approach [6] and the proposed ship detectors for detecting a ship signal is compared. In the experiment, one particular CPI of dataset 2 was processed by each detector 100 times to reduce measurement fluctuations of the processing server. The processing time per detector was then averaged.

The proposed detector in Doppler domain achieved a processing time of 0.088 s whereby the detector outperforms the CFAR-based detector with a processing time of 0.824 s. It has to be pointed out that the proposed Faster R-CNN ship detectors were designed for GPU, while the CFAR-based method was designed for CPU. Besides, the proposed detectors could be further optimized in terms of processing time by replacing the ResNet-50 [12] with a smaller CNN as the backbone of the Faster R-CNN models.

## VI. Conclusion

This letter presents two novel object-oriented ship detectors based on the Faster R-CNN deep learning framework. The ship detectors are trained and tested using eleven real X-band RC radar datasets acquired by DLR's airborne systems F-SAR and DBFSAR. The first ship detector operates on RC radar data in time domain, while the second ship detector operates in Doppler domain. Both detectors were able to detect all the AIS carrying ships contained in the testing datasets, achieving high $r$ values even in complex scenarios with several man-made objects. Compared to the state-of-the-art CFAR-based method from [6], which operates in Doppler domain, the proposed ship detector in Doppler domain was able to provide less false detections and reduced processing time. Nevertheless, it has to be pointed out that a bias in the precision $p$ and the $F_1$-score may be expected since the detections obtained from potential ship objects without AIS transponder are assumed as FP.

## References

[1] *Revised Guidelines for The Onboard Operational Use of Shipborne Automatic Identification Systems (AIS)*, Int. Maritime Org., London, U.K., 2015, pp. 1–17.
[2] H. Greidanus, "Satellite imaging for maritime surveillance of the European seas," in *Remote Sensing of the European Seas*. Dordrecht, The Netherlands: Springer, 2008, pp. 343–358.
[3] A. Moreira, P. Prats-Iraola, M. Younis, G. Krieger, I. Hajnsek, and K. P. Papathanassiou, "A tutorial on synthetic aperture radar," *IEEE Geosci. Remote Sens. Mag.*, vol. 1, no. 1, pp. 6–43, Mar. 2013.
[4] M. F. Fingas and C. E. Brown, "Review of ship detection from airborne platforms," *Can. J. Remote Sens.*, vol. 27, no. 4, pp. 379–385, 2001.
[5] D. J. Crisp, "The state-of-the-art in ship detection in synthetic aperture radar imagery," Defence Sci. Technol. Organisation Inf. Sci. Lab., Edinburgh, U.K., Tech. Rep. DSTO-RR-0272, 2004.
[6] S. K. Joshi, S. V. Baumgartner, A. Barros Cardoso da Silva, and G. Krieger, "Range-Doppler based CFAR ship detection with automatic training data selection," *Remote Sens.*, vol. 11, no. 11, pp. 1270–1305, 2019.
[7] F. Sharifzadeh, G. Akbarizadeh, and Y. Seifi Kavian, "Ship classification in SAR images using a new hybrid CNN–MLP classifier," *J. Indian Soc. Remote Sens.*, vol. 47, pp. 551–562, Oct. 2019.
[8] T. Hoeser, F. Bachofer, and C. Kuenzer, "Object detection and image segmentation with deep learning on Earth observation data: A review—Part II: Applications," *Remote Sens.*, vol. 12, no. 18, pp. 3053–3099, 2020.
[9] X. X. Zhu et al., "Deep learning meets SAR: Concepts, models, pitfalls, and perspectives," *IEEE Geosci. Remote Sens. Mag.*, vol. 9, no. 4, pp. 143–172, Dec. 2021.
[10] S. Ren, K. He, R. Girshick, and J. Sun, "Faster R-CNN: Towards real-time object detection with region proposal networks," *IEEE Trans. Pattern Anal. Mach. Intell.*, vol. 39, no. 6, pp. 1137–1149, Jun. 2017.
[11] X. Leng, J. Wang, K. Ji, and G. Kuang, "Ship detection in range-compressed SAR data," in *Proc. IEEE Int. Geosci. Remote Sens. Symp. (IGARSS)*, Jul. 2022, pp. 2135–2138.
[12] K. He, X. Zhang, S. Ren, and J. Sun, "Deep residual learning for image recognition," in *Proc. IEEE Conf. Comput. Vis. Pattern Recognit. (CVPR)*, Jun. 2016, pp. 770–778.
[13] A. Reigber et al., "Very-high-resolution airborne synthetic aperture radar imaging: Signal processing and applications," *Proc. IEEE*, vol. 101, no. 3, pp. 759–783, Mar. 2013.
[14] A. Reigber et al., "Current status of DLR's new F-SAR sensor," in *Proc. 8th Eur. Conf. Synth. Aperture Radar (EUSAR)*, Jun. 2010, pp. 1078–1081.
[15] A. Reigber et al., "The high-resolution digital-beamforming airborne SAR system DBFSAR," *Remote Sens.*, vol. 12, no. 11, p. 1710, 2020.
[16] T.-Y. Lin et al., "Microsoft COCO: Common objects in context," in *Proc. Eur. Conf. Comput. Vis. (ECCV)*, 2014, pp. 1–15.
[17] J. Jiao et al., "A densely connected end-to-end neural network for multiscale and multiscene SAR ship detection," *IEEE Access*, vol. 6, pp. 20881–20892, 2018.